Tellus (1985), *37A*, 433–450. Polar Low Special Issue

Satellite climatological aspects of the "polar low" and "instant occlusion"

By ANDREW M. CARLETON, *Department of Geography, Arizona State University, Tempe, AZ 85287, U.S.A.*

(Manuscript received November 15; in final form April 24, 1985)

ABSTRACT

Middle resolution DMSP (Defense Meterological Satellite Program) visible and infrared imagery are analyzed in conjunction with surface and upper-air synoptic observations for two years' (1977, 1978/79) mid-season months (January, April, July, October) to derive synoptic climatological information on the "polar low" and "instant occlusion" phenomena. Polar-air vortices occur most frequently over the oceans in winter. Regional differences in the dominance of cloud signature sub-types confirm variations in the dynamics involved in polar-air cyclogenesis, as noted by previous workers. The "comma cloud" appears to occur more frequently in the North Pacific, while the spiraliform vortex predominates in the North Atlantic. The latter seems to be at least partly attributable to the effect of the eastern Arctic sea-ice boundary, as demonstrated by an analysis of imagery for two winters (D, J, F), each representative of an opposing mode of the North Atlantic Oscillation (1974/75, 1976/77).

Composite synoptic "models" of polar lows reveal surface-pressure departures similar to those for cyclogenesis of the frontal wave type. However, a cold core and little vertical tilt distinguish the polar low in the mean. The "instant occlusion" exhibits surface-pressure departures that are deeper and comparable to the mature/dissipating stages of wave cyclone evolution. Spatial patterns of the upper-air anomalies associated with instant occlusions show two distinct vortices: one apparently derived from the polar low, the other from the incipient frontal wave with which it has merged. The seasonal and latitude-dependent cyclone intensity statistics (all types) are applied to the cloud vortex inventory of the North Atlantic–Europe sector for January 1979. The results support the rôle of the polar low as a synoptic indicator of anomalous winter circulation in the extratropics.

1. Introduction

The operational analysis of satellite cloud imagery has long recognized the existence of signatures of extratropical cyclogenesis which differ substantially from the Norwegian frontal-wave model (Reed, 1979). Many of these systems develop in the cold air to the rear of major frontal cyclones (e.g. Troup and Streten, 1972; Chang and Sherr, 1969), and are frequently characterized by a distinct "comma cloud" vortex (e.g. Lyall, 1972; Reed, 1979). The collective term "polar low" has been used to describe this cyclogenesis. However, higher resolution imagery shows that a multitude of configurations for polar-air vortices spanning the meso-alpha range (100–1000 km) is possible. These include spiraliform vortices that resemble mini-tropical cyclones (Rasmussen, 1981), multiple ("merry-go-round") vortices, and banded formations of varying cloud depths (Oerlemans, 1980; Forbes and Lottes, 1982). Such variety implies differences in the formation dynamics that range from the shallow baroclinic wave of Harrold and Browning (1969) and others (Mansfield, 1974; Duncan, 1977; Mullen, 1979) to the dominantly thermal-barotropic origin involving CISK (Økland, 1977; Rasmussen, 1979), or a combination of the two but with different relative contributions depen-

dent upon either the region of formation (Sardie and Warner, 1983) or stage of development (Forbes and Lottes, 1985). Additional physical mechanisms to account for polar air cyclogenesis include interactions between incipient comma clouds and the cloud bands of the subtropical jet stream (Thepenier and Cruette, 1981), the evolution of multiple commas from pre-existing old cyclonic circulations (Zick, 1983), and the interaction between post-frontal cold-air cloud masses and the polar front that results in the so-called "instant occlusion" (e.g. Mullen, 1983). Very little is known about the instant occlusion phenomenon (Carleton, 1981a), although studies related to the CYCLES (cyclonic extratropical storms) project (Locatelli et al., 1982) suggest that it may be a rather common form of cyclogenesis over the North Pacific in winter. The explosive extratropical cyclogenesis ("bomb") events described by Sanders and Gyakum (1980) and observed dominantly in connection with frontal waves (Murty et al., 1983), have been shown to also involve some polar low and instant occlusion developments in the North Pacific (Mullen, 1983).

An adequate composite picture of the synoptic environments in which polar air vortices develop is only now beginning to emerge (e.g., Forbes and Lottes, 1985). The development of a polar low climatology for the northern hemisphere is similarly at an early stage (Reed, 1979; Forbes and Lottes, 1982), although it seems these systems may signify anomalous extratropical circulation. The present paper presents synoptic climatological aspects of "polar lows" and "instant occlusions" derived from analysis of sets of middle resolution DMSP (Defense Meteorological Satellite Program) imagery. Included are a two-year mid-season climatology of these cloud vortex types, the relationship of polar-air vortices to sea ice-extent variations in the eastern Arctic for two case winters representative of opposing phases of the North Atlantic Oscillation (NAO), and statistical models of the structure of the polar low and instant occlusion obtained from compositing surface and upper-air synoptic data. Differences in the relative dominance of moist baroclinic and CISK processes to polar low development between the North Pacific and Atlantic have been suggested (Sardie and Warner, 1983). Preliminary corroboration of these climatological differences using the satellite data can now be given.

2. Data and methods of analysis

2.1. DMSP imagery

Twice-daily infrared (8–13μm) mosaics for the northern hemisphere, derived from the DMSP polar-orbiting system, are obtained for two years' mid-season months (January 1978, 1979; April 1977, 1978; July 1977, 1978; October 1977, 1978) and for the two NAO winters (DJF) of 1974/75 and 1976/77. The imagery have a resolution of 3.7 km and are mapped at a nominal scale of 1:30 M on a mylar half-hemispheric polar stereographic base. Equatorial crossing times of the satellites, necessary for comparing the cloud vortex type and location with synoptic observations, are given for the individual swathes comprising each mosaic. Fig. 1 is an example of part of a mosaic for the North Atlantic in January 1979, and shows several polar air vortices to the west of a major wave cyclone.

2.2. Cloud vortex classification system

The occurrence of polar air cloud vortices was determined using a genetic classification system developed specifically for the higher resolution imagery now available. The full scheme is presented in Carleton (1985) where it is used to derive a seasonal climatology of the interactions between the synoptic circulation and cryosphere extent in the northern hemisphere. The scheme builds upon the synoptic classification systems proposed earlier by Widger (1964), Chang and Sherr (1969) and Troup and Streten (1972), but is more detailed at the secondary and tertiary levels of classification (refer Fig. 2). The distinction between cyclonic formation on a frontal cloud band and non-frontal (polar air) development was retained (Fig. 2) for both the initial ("cyclogenetic"-A) and "developing" (B) categories of cyclonic evolution. However, with the onset of maturity (C-vortices), signatures of both frontal and non-frontal origin appear sufficiently similar and were grouped together. The major cyclogenetic vortices are the frontal wave (A1), the polar low (A2) and the instant occlusion (A3) (Fig. 2). Three sub-categories of the A2 type are recognized: the comma cloud in isolation (A2i), the spiral polar low (A2ii), and the polar vortex that develops from an old cyclonic circulation (A2iii). The A3 (instant occlusion) was taken to be the vortex resulting from the initially-observed merger between the rear-zone comma cloud and the frontal

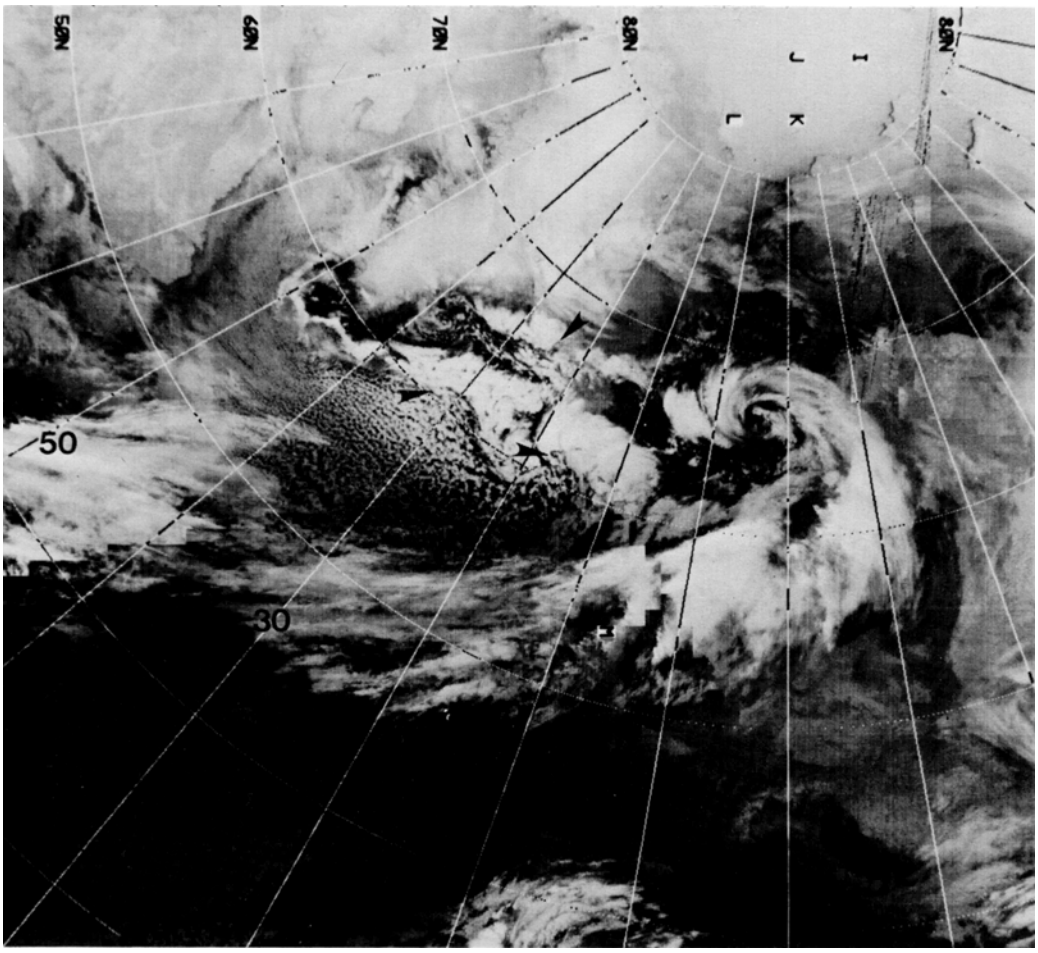

Fig. 1. DMSP infrared mosaic for the North Atlantic/Europe sector (January 1979). Arrows indicate centers of polar low vortices (at 61° N, 34° W; 62° N, 17° W; 66° N, 25° W). Letters on the images identify orbital swaths used to compile the mosaic.

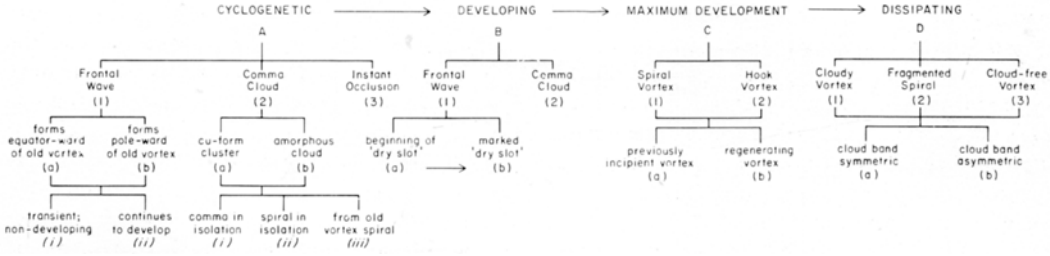

Fig. 2. Part of the classification system developed for cloud vortices appearing in higher resolution visible and infrared satellite imagery and presented in full in Carleton (1985).

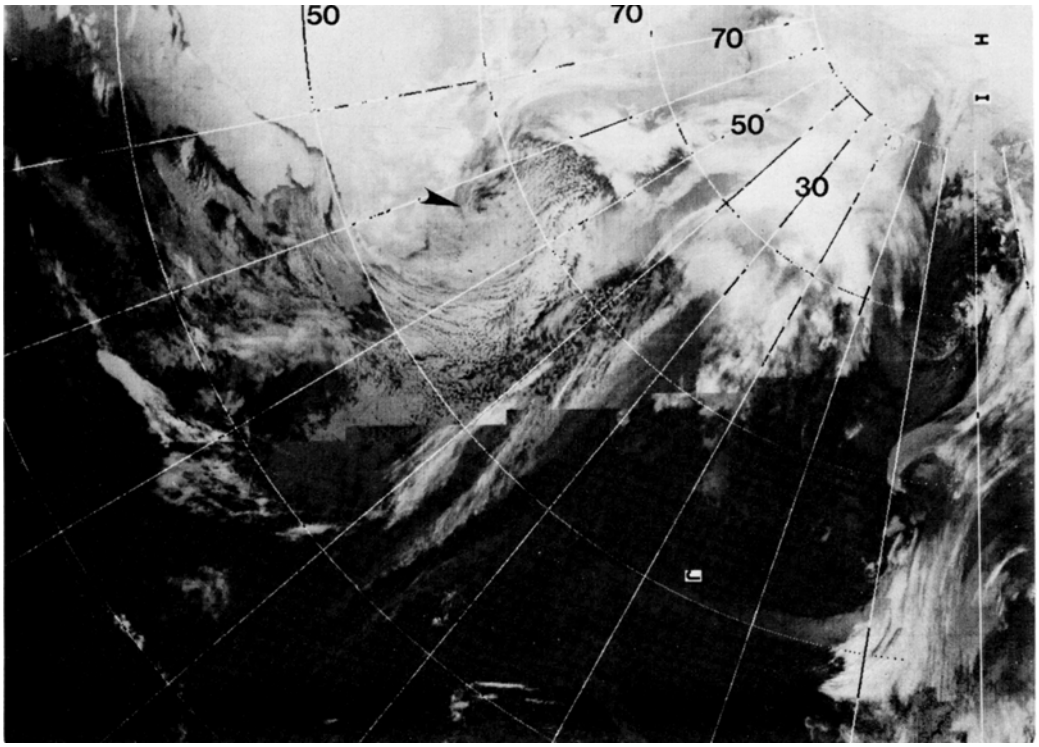

Fig. 3. DMSP images of polar air vortices: (a) type A2ii (spiral) forming near the Newfoundland/Labrador coast in January 1979 (57° N, 57° W), and developed into the comma cloud (Type B2) in (b) at 57° N, 51° W. The arrow in (a) points to the center of the cloud vortex.

band. The appearance of either a "dry slot" or tight spiral associated with the polar air vortex was considered evidence of continued development and the transition to stage B.

Examples of cloud vortex types are given in Figs. 3 and 4. The spiral polar low (A2ii) in Fig. 3a developed into the tight comma vortex (type B2) shown in Fig. 3b. The sequence of images in Fig. 4a–c denotes typical stages in the development of an instant occlusion (A3) vortex. While additional A2 sub-categories could have been recognized (see Forbes and Lottes, 1982, 1985), the three accommodated in the present classification were considered to represent the most distinct configurations for polar air vortices that continued to develop over both the North Pacific and Atlantic oceans.

2.3. US Navy "Spot" and N.M.C. climatological grid-point data.

Synoptic climatological models of polar low, instant occlusion and frontal-wave cyclogenesis were derived using large numbers of surface and upper-air synoptic observations (on tape), primarily for the oceans and adjacent land areas. US Navy "Spot" synoptic reports were available (after editing) at one-hourly and three-hourly intervals respectively for surface ship and land stations. Upper-air observations were available every 12 hours (00GMT, 12GMT) and extracted for the 850, 700, 500 and 300 mb levels for this study.

Long-term monthly mean surface pressure and geopotential height data for the Northern Hemisphere are available for 5° latitude/longitude grid points on magnetic tape. These data constitute those used in the climatology of Crutcher and Meserve (1970).

2.4. Derivation of synoptic cloud vortex models

A cloud vortex model was obtained by extracting all available surface and upper-air observations

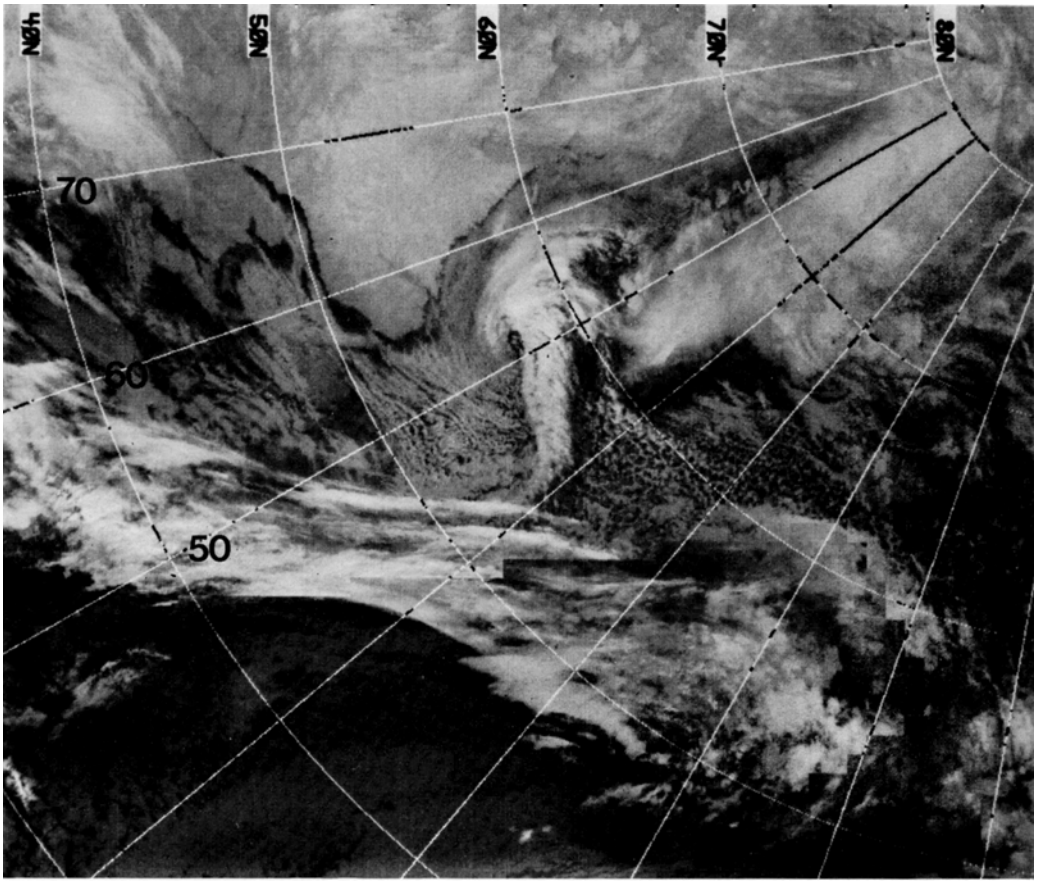

Fig. 3b.

within the range of influence of an individual vortex, expressing each as a departure from the climatological mean interpolated to the nearest 5° latitude/longitude grid point for that month and level, and computing mean monthly anomaly patterns ($\overline{\Delta p}$, $\overline{\Delta h}$) by compositing for a particular vortex type. This procedure, depicted schematically in Fig. 5, is similar to that used by Troup and Streten (1972) for determining the synoptic characteristics of southern hemisphere cloud vortices. However, the far greater availability of observations and the use of a computer program in the present study enables more detailed investigation of composite cloud vortex structure for the major classification types. For an individual vortex (Fig. 5a) the area of influence is taken arbitrarily to be the radius (r: °latitude) eastward from the center to the cloud band, plus 2° for vortices $r = 1, 2, 3°$; $r+3°$ for vortices of radius 4 through 7°, and $r + 4°$ for vortices of 8°. Very few cyclones exhibit radii larger than 8° of latitude. In order to obtain sufficient upper-air reports, a linear interpolation routine locates the vortex between two twelve-hourly synoptic periods to the nearest hour (Fig. 5a).

Mean monthly pressure/height anomaly patterns (Fig. 5b) were computed by averaging all individual observations with respect to the mean vortex center ($\bar{X}$) over 60° azimuthal sectors, overlapping by 30°, and for radial bands 0–3°, 4–7° and 8–10°. The sector mean departures ($\overline{\Delta p}$, $\overline{\Delta h}$) were then used to derive spatial anomaly patterns of vortex types in Fig. 10, or alternatively, whole-vortex anomalies ($\overline{\Delta w}$) and central pressure ($\overline{\Delta c}$)

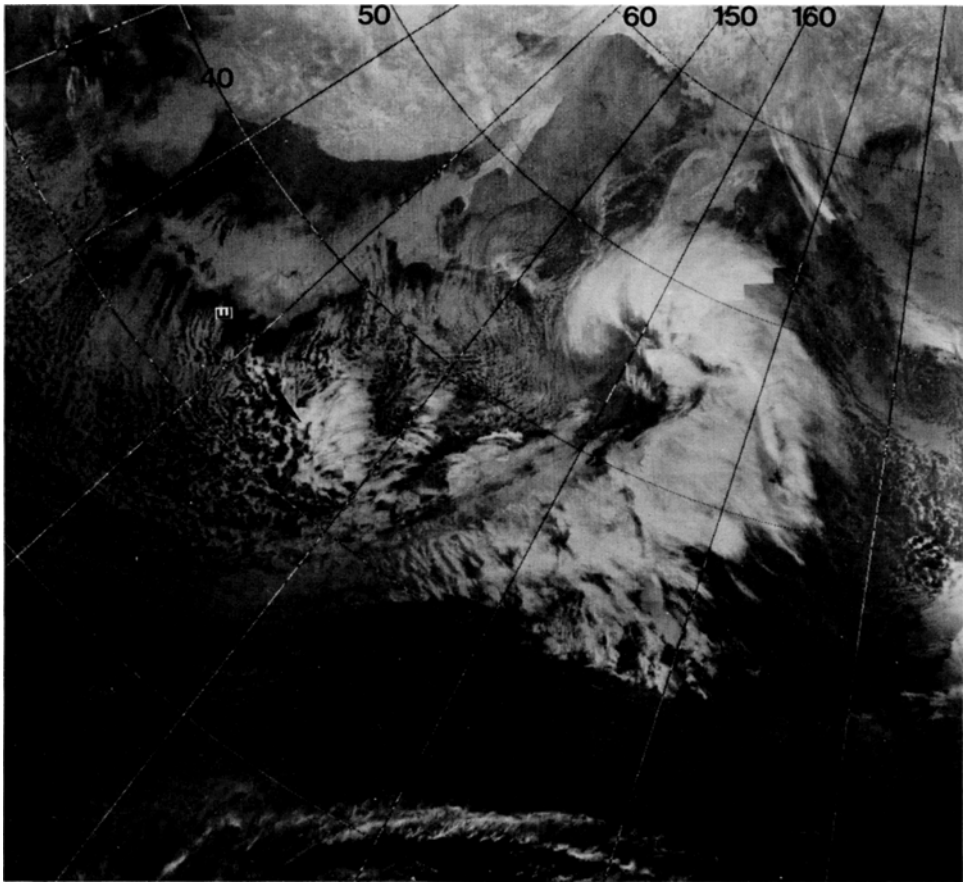

Fig. 4. DMSP sequence of an "instant occlusion" over the western North Pacific at approximately 12-h intervals (arrows indicate cloud vortex center): (a) separate polar air (A2i) vortex at 33° N, 146° E advances towards an incipient frontal wave (A1a) at 38° N, 155° E. (b) interaction between the two cloud vortices (36° N, 164° E). (c) resulting cloud vortex (45° N, 177° E) having a configuration typical of dissipating frontal wave systems.

statistics. Latitudinal variations in cyclone intensity were also computed (not shown) by expressing the average vortex anomaly in each 10° zone as a departure from the standard (all-latitudes) models given in Table 3.

Shortcomings with the compositing technique involve the inclusion of polar low vortices of all configurations and sizes (partly compensated for by the spatial averaging procedure) from both the North Pacific and Atlantic oceans. However, since comparatively little is known about the polar low, compositing is justified as a first approximation to the overall climatological character of these vortices and to show how they differ from other cloud vortex types (*viz.* Troup and Streten, 1972; Streten and Kellas, 1973). The models are not intended as a substitute for detailed case studies of polar lows, but to provide a conceptual climatological framework (see also Forbes and Lottes, 1985). As such, it has been suggested (Forbes, personal communication) that polar lows are indicative of anomalous circulation patterns with 500 mb heights that are well below normal. A preliminary examination of this relationship is possible here using the seasonal and latitude-dependent surface pressure and height ($\overline{\Delta p}$, $\overline{\Delta h}$) model statistics

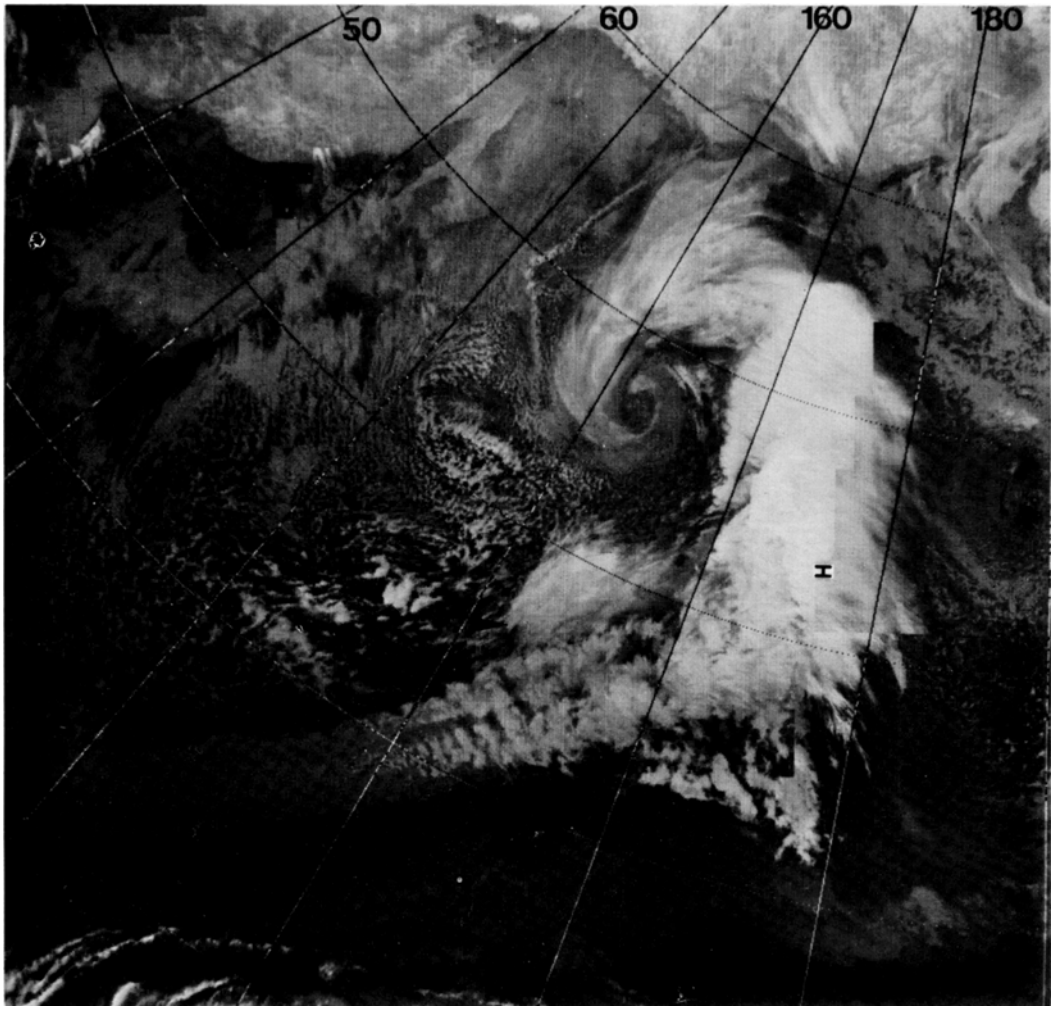

Fig. 4b.

derived for each key signature type and applied to the cloud vortex census for January 1979. This month was anomalous in the severity of winter weather over western and northern Europe and the extent of sea ice in the Baltic. The $\overline{\Delta p}$ and $\overline{\Delta h}$ values were assigned to the twice-daily DMSP observations of all cloud vortex types and anomalies were accumulated ($\sum\overline{\Delta p}$, $\sum\overline{\Delta h}$) in each 10° latitude and longitude unit for the entire month. This procedure produces a cyclonic activity index dependent not only on the frequency of a particular vortex type but on its statistical intensity. The latter is a function of mean vortex size, atmospheric level, latitude , and season of occurrence. This method of accumulating pressure/height anomalies develops that used by Streten (1975) in a satellite study of the synoptic-scale response of the atmospheric circulation in the South Pacific to the Southern Oscillation. While this statistical intensity approach is an improvement on the use of cyclone frequency data, the resulting anomaly maps should be considered an approximation to reality (Streten, 1975) that awaits more detailed analysis subsequently.

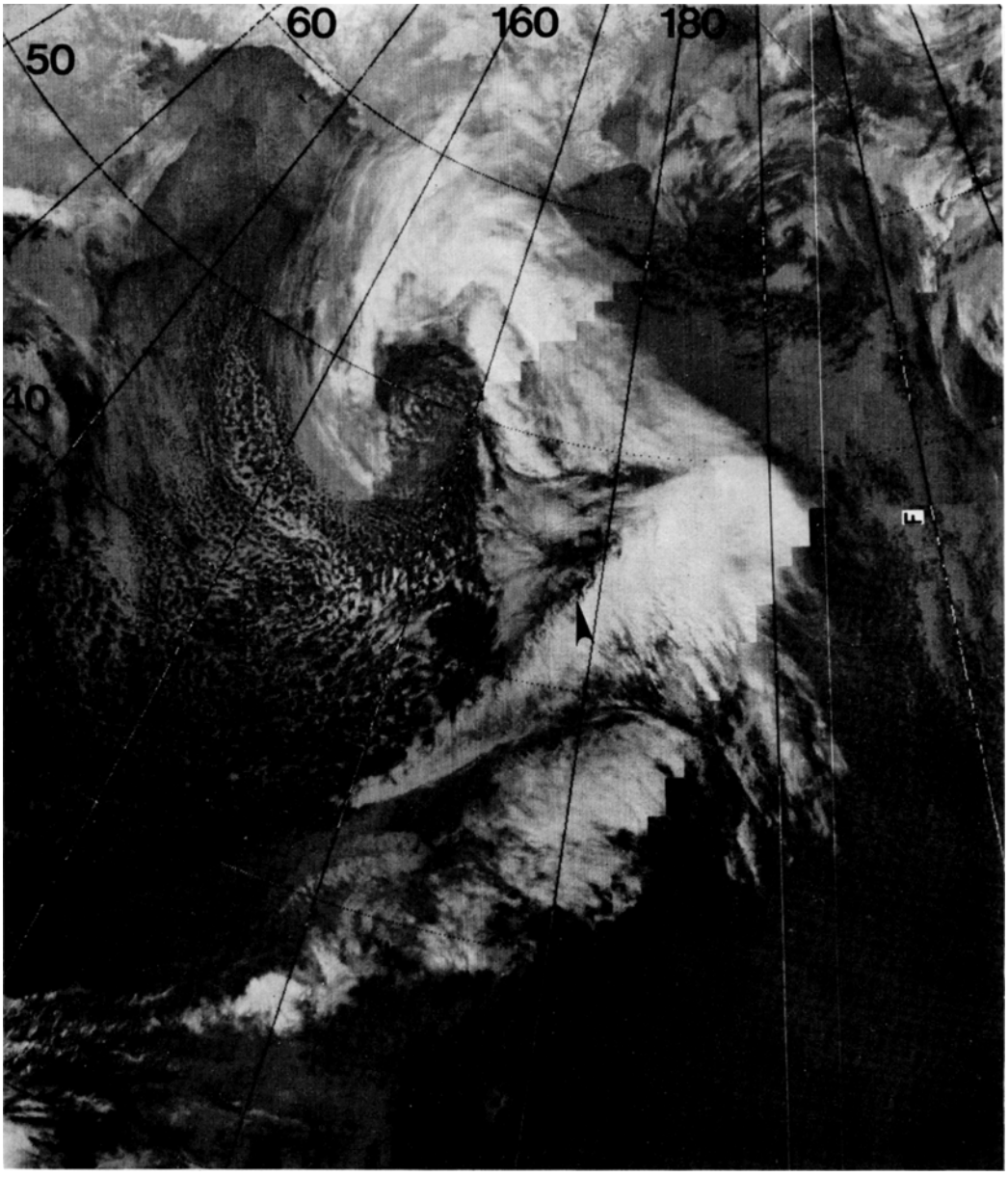

Fig. 4c.

3. Mid-season climatology of polar lows and instant occlusions

Multi-year satellite climatologies of polar low (principally comma cloud) and "instant occlusion" vortices have been available for the southern hemisphere oceans for some time (Streten and Troup, 1973; Carleton, 1979, 1981a, b). Similar studies for the northern hemisphere have been slower to appear, due to the greater availability

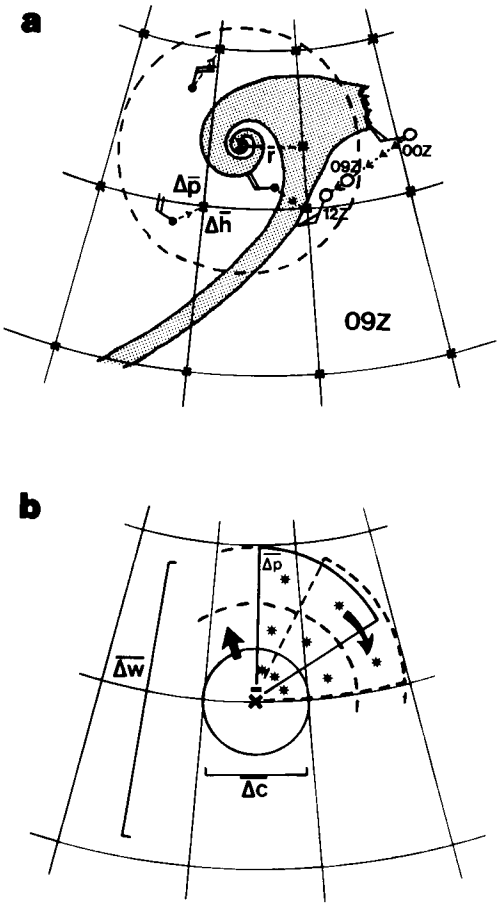

Fig. 5. Schematic diagrams showing the derivation of synoptic climatological cloud vortex models (refer text).

of conventional meteorological data for weather analysis and forecasting. However, a mid-season climatology of the successive stages of cloud vortex evolution has recently been presented by Carleton (1985). The polar low has been studied for the North Pacific by Reed (1979), and for a shorter period for the North Atlantic by Forbes and Lottes (1982). Rabbe (1975) notes the predominance of polar air vortices affecting Norway in wintertime.

Table 1 shows the two-year hemispheric daily mean occurrences of polar low (types A2, B2) and instant occlusion (A3) vortices, and compares them with cyclogenesis of the frontal wave (A1, B1) type. Cyclogenesis predominates over the northern hemisphere oceans in all seasons except summer, at which time the thermal contrasts at the land-ocean boundary figure prominently (see Carleton, 1985). While frontal wave cyclogenesis is seasonally uniform (Table 1), the incidence of polar lows peaks in winter (*viz.* Reed, 1979). This is probably due largely to enhanced thermal contrasts between the ocean surface and the atmosphere during winter cold air outbreaks (see, e.g., Houghton, 1958). Accordingly, polar lows decrease in frequency through the spring to a summer minimum (Table 1), although cyclonic activity (all types) exhibits a minimum in the spring. Instant occlusion vortices constitute only a small percentage of the total number of cyclones for the hemisphere (Table 1). They also exhibit a summer frequency minimum, with the greatest occurrences in autumn (October) and winter, at least for the two years studied here.

The polar low vortices (type A2) are stratified in Table 2 according to the three sub-types (A2i, A2ii,

Table 1. *Mean daily frequencies of frontal wave (A1, B1), polar low (A2, B2), and instant occlusion (A3) cloud vortices for the northern hemisphere, two years' mid-season months (all latitudes)*

	Vortex type					
	Cyclogenetic			Developing		mean daily total (cloud vortices of all types)
	frontal wave (A1)	polar low (A2)	instant occlusion (A3)	frontal wave (B1)	polar low (B2)	
January	2.4	2.1	0.2	2.9	0.8	16.7
April	2.2	0.6	0.1	2.3	0.3	11.7
July	2.0	0.2	0	2.6	0.1	12.5
October	2.1	1.0	0.2	2.9	0.6	14.9

(From Carleton, 1985)

Table 2. *Frequencies of incipient polar air vortex types (A2i, A2ii, A2iii) for North Pacific and North Atlantic/Europe sectors: January (1978, 1979)*

	A2i		A2ii		A2iii	
	incipient comma cloud		spiral polar low		polar low from pre-existing cyclonic circulation	
	Pacific	Atlantic	Pacific	Atlantic	Pacific	Atlantic
January 1978	32	26	19	47	5	4
January 1979	55	33	11	16	0	3
TOTALS	87	59	30	63	5	7

A2iii) for the North Atlantic and North Pacific sectors in January (two years). The data indicate a predominance of the incipient comma cloud formation (A2i) in the North Pacific but a greater frequency of the spiraliform type (A2ii) in the North Atlantic. This appears to offer observational confirmation of the findings of Sardie and Warner (1983), that moist baroclinic processes dominate in polar low formation for the North Pacific, but that CISK is of additional importance for North Atlantic polar-air cyclogenesis (see also Rasmussen, 1979, 1981; Forbes and Lottes, 1985). The extension of the open ocean to higher latitudes in the North Atlantic compared with the North Pacific is probably crucial in explaining these differences, and for the observed relationship between cyclonic activity and the Greenland/Norwegian Sea ice margin in winter (Carleton, 1985). A similar case has been made for certain sectors of the high-latitude South Pacific (Carleton, 1981b). There is no clear regional disposition of polar air vortices which evolve from pre-existing cyclonic circulations (type A2iii), at least for the two years investigated here (Table 2). Their frequency of occurrence is considerably less than for the A2i and A2ii types and this is also consistent with the study of Forbes and Lottes (1985).

Latitudinal frequencies of cyclogenetic and developing cloud vortices (A1, A2, A3, B) for January are given in Fig. 6 which shows that most frontal wave cyclogenesis (A1) occurs between 30–50° N while incipient polar lows (A2) predominate between about 40–60° N. These patterns are not as distinctly differentiated latitudinally as in the southern hemisphere (Streten and Troup, 1973; Carleton, 1979), however, this may be at least partly explained by the effect of averaging around the hemisphere. Thus, regional variations in the dominant latitude of a particular vortex type are smoothed out. The latitude distribution of the instant occlusion (A3) appears intermediate to those shown for A1 and A2 (about 30–60° N), and is to be expected when considering it results from the merger of these two vortex types (e.g. Locatelli et al., 1982). This is consistent with the situation

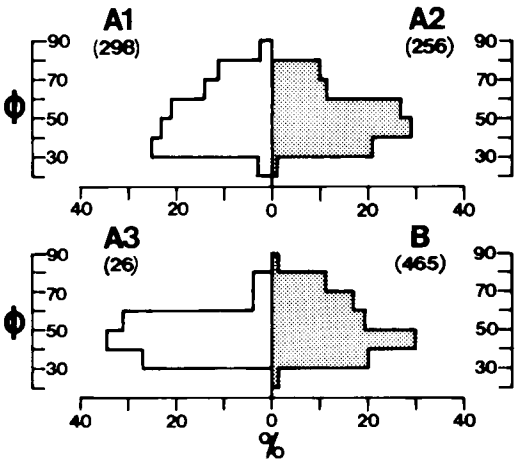

Fig. 6. Latitude frequencies of cyclogenetic (A) and developing (B) cloud vortices in January (combined 1978, 1979). The types shown are A1 (incipient frontal wave); A2 (incipient polar low), A3 (instant occlusion), and B (combined B1 and B2). Frequencies in each 10° latitude band are presented as the % of the total hemispheric number (in brackets) of that type over all latitudes.

noted for instant occlusions in the southern hemisphere (Carleton, 1981a).

The presence of a latitudinal ocean temperature gradient enhanced by an ice edge is suggested by Sardie and Warner (1983) as being a dynamic factor influencing polar low development in the North Atlantic. It might explain the relatively high frequencies of these vortices noted for that region in winter (Rabbe, 1975; Økland, 1977). The extent to which sea ice variations, forced by atmospheric and oceanic anomalies, may feed back to influence cyclogenesis near the ice edge is examined here for two winters (D, J, F) representative of opposing modes of the North Atlantic Oscillation (NAO). The NAO has been defined (van Loon and Rogers, 1978) as an opposition in sign ("seesaw") of the temperature anomaly Oslo–Jakobshavn equal to or greater than 4° C from the long-term mean. The two key see-saw states (Greenland Below: GB, and Greenland Above: GA) are represented here respectively by the winters of 1974/75 and 1976/77. GA and GB temperature anomalies in the North Atlantic are manifestations of statistically-significant differences in sea-level pressure, related partly to the Icelandic mean low, the zonal component of the geostrophic wind and planetary long waves.

Fig. 7 shows satellite-observed total cloud vortex frequency differences between the two winters (GB minus GA). The opposition apparent between Greenland-western Europe and western North America-Aleutians confirms the multi-year GB and GA surface pressure composites given by van Loon and Rogers (1978). Also evident is the opposition in sign, for a given see-saw mode, between the Icelandic and Aleutian lows. This is reflected in the ice-extent variations of the Arctic marginal seas, which involve heavy (light) ice in Davis Strait and the Bering Sea in winter 1975 (1977) and light (heavy) ice on the Barents and Okhotsk seas in 1975 (1977).

The latitude/longitude distributions of frontal wave (A1) and polar low (A2) cyclogenesis for the North Atlantic sector (80° W–50° E) are given in Fig. 8. In both winters, the dominant zone of frontal cyclogenesis is seen to lie over middle latitudes. The higher frequency of polar lows (A2) over middle latitudes in 1976/77 (GA) is related to the anomalous cold air excursions southward over the north-east Atlantic/Europe region between about 40–60° N compared with 1974/75. A subsidiary zone of A2 cyclogenesis, related to the sea-ice edge, can be seen for both winters in the peaks in frequency for the 70–75° N zone (Fig. 8). This is particularly marked in the GB (1975) winter. Examination of the longitudinal distribution of these vortices for the 60–80° N band (Fig. 8) shows a peak eastward of about 15° W (i.e. they form in association with the sea ice boundary of the Greenland/Norwegian seas which does not change much between NAO modes). Carleton (1985) demonstrates this ice-edge–cyclogenesis effect synoptically (his Fig. 12).

Fig. 8 indicates the importance of the Norwegian Sea for the rapid modification of southward-moving Arctic airstreams in winter (Gagnon, 1964; Økland, 1976) and for the subsequent appearance of polar lows, related partly to CISK (Forbes and Lottes, 1985), at the northern coast of Norway (Rabbe, 1975; Økland, 1977; Rasmussen, 1979). Conversely, strong differences in the frequency of polar low cyclogenesis occur in association with the larger NAO sea ice extent variations in Davis Strait. More extensive ice in winter 1975 is associated with greater frequencies of polar lows in the 50–60° N zone between 60–40° W compared with the same zone in 1977. These cyclogenesis increases are conceivably the result of feedback to the atmosphere by the heavy regional sea ice conditions, which are in turn related to the anomalously deep Icelandic low in that year (Fig. 7). Additional cases are required to confirm these preliminary ice edge–polar-air cyclogenesis results.

4. Synoptic-climatological models of polar lows and instant occlusions

The surface pressure, upper-air height and 850–700 mb thickness anomaly statistics associated with polar low vortices are composites of all three signature sub-groups (A2i, A2ii, A2iii) for both the North Pacific and North Atlantic–Europe sectors (refer Data and Methods, Section 4). Since the comma cloud (A2i) is considerably the more numerous for the hemisphere as a whole (Table 2), the models should be considered most closely representative of that vortex type. They are broadly comparable with statistics for polar lows over the southern hemisphere oceans (Troup and Streten, 1972), and for the North Atlantic derived using a different method by Forbes (personal communication).

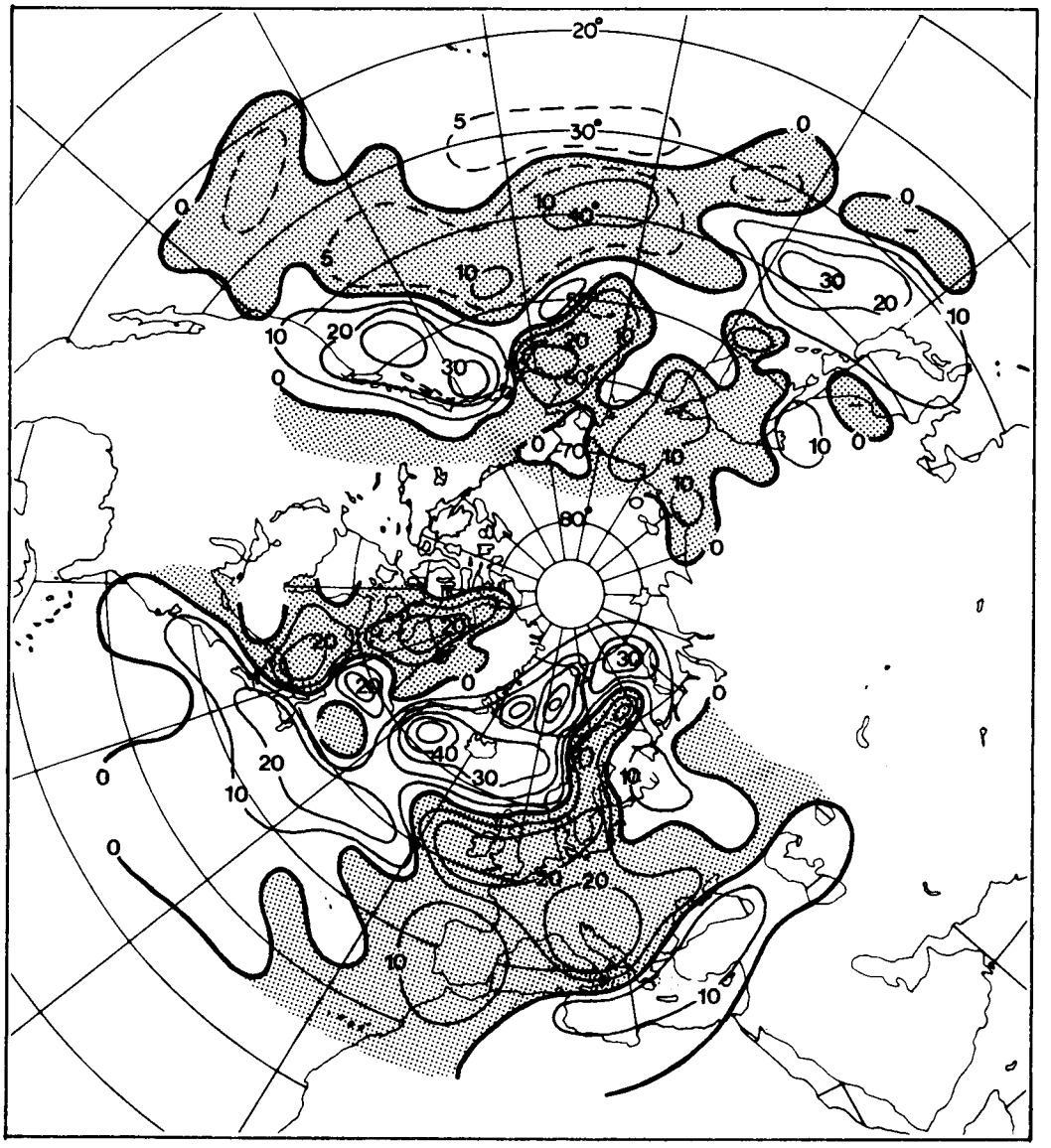

Fig. 7. Difference map (winter 1975 minus winter 1977) of total cloud vortex frequencies (all types) as determined from twice-daily DMSP imagery. Cyclone frequencies in each 5° latitude/10° longitude unit are area-normalized to 45° N and isoplethed. Shaded areas indicate negative frequencies (1977 greater than 1975).

Table 3 shows the mean SLP and 500 mb height anomalies for all major cyclonic vortex signature types in January. There is a general increase in intensity (increasingly negative anomalies) through the evolution sequence that is similar to that determined for vortices in the southern hemisphere by Troup and Streten (1972). Standard deviations are generally high and reflect the inclusion of vortices over all latitudes poleward of 20°N. Surface pressure anomalies are similar (about −7 mb) for the frontal wave (A1) and polar low (A2) model types, but the instant occlusion is considerably deeper (−10 to −14 mb) and is comparable to the mature (C-stage) cloud vortices. The biggest

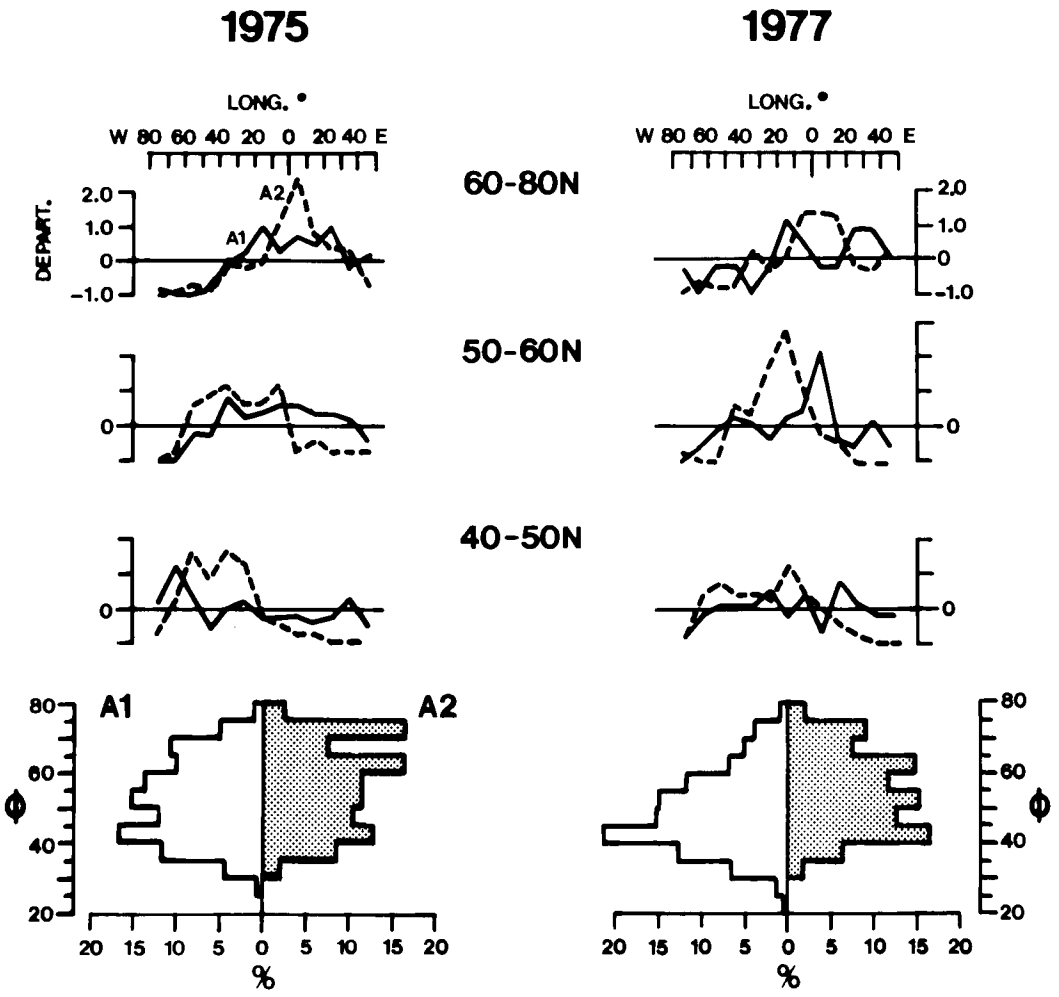

Fig. 8. Longitude distribution of satellite-observed cyclogenesis (frontal wave: A1; polar low: A2) in three latitude zones for the North Atlantic sector (80° W–50° E) in winters (D, J, F) of 1975 and 1977. Values in each 10° longitude sector are presented as the fractional departure from the mean ('0' reference line) for the vortex type in that latitude zone. The lower half of the diagram shows latitude frequencies of each cyclogenesis for the North Atlantic sector.

differences between A1 and A2 cyclogenetic types, however, are found in the upper air. Both the incipient (A2) and developing (B2) polar lows and the instant occlusion (A3) exhibit a cold-core structure at middle levels that is substantially deeper than the frontal wave (A1) and compares more with dissipating (D-stage) cyclones. These differences reflect the preponderance of comma cloud types in the polar low models, and the dominance of warm air advection east of the centers of incipient frontal wave systems. This is further demonstrated in Fig. 9, which shows west–east transects of the composite 850–700 mb thickness anomalies. The marked asymmetry of the frontal wave (A1, B1) types (cf. A2 and A3) is apparent. Thickness advection appears to be less dominant a mechanism in the formation of most polar lows (Forbes and Lottes, 1985) compared with frontal wave cyclogenesis.

Spatial patterns of the all-latitudes model anomalies for October 1977 (Fig. 10) highlight the structural differences between frontal wave and

Table 3. *Summary statistics of SLP (mb) and 500 mb height (m) anomalies (in brackets) in specified annular bands for standard (all-latitudes) cloud vortex types in the northern hemisphere: January*

	Radial range (° of latitude from vortex center)					
	1–3° (central pressure)			4–6°		
Vortex type	Mean	S.D.	no. of vortices	Mean	S.D.	no. of vortices
incipient frontal wave	−7.2	10.4	42	−4.7	10.3	42
(A1)	(−39.7)	(113.1)	(26)	(−30.0)	(111.1)	(24)
incipient polar low	−6.0	8.7	45	−6.4	7.6	35
(A2)	(−129.6)	(61.4)	(26)	(−150.4)	(82.2)	(15)
instant occlusion	−10.6	7.7	6	−13.7	7.9	7
(A3)	(−140.7)	(67.0)	(3)	(−151.8)	(77.8)	(7)
developing frontal wave:	−8.1	10.2	39	−7.5	10.3	33
initial dry slot (B1a)	(−33.9)	(88.4)	(15)	(−44.6)	(123.1)	(18)
fully formed dry slot	−12.9	10.0	23	−10.5	9.2	23
(B1b)	(−129.6)	(95.6)	(11)	(−72.7)	(95.2)	(19)
developing polar low	−7.9	11.1	19	−10.0	6.3	16
(B2)	(−127.0)	(77.0)	(8)	(−109.5)	(107.7)	(5)
mature hook vortex	−15.9	8.6	34	−10.8	8.3	38
(C2)	(−100.9)	(65.1)	(20)	(−77.3)	(105.6)	(27)
mature spiral vortex	−20.5	9.7	19	−15.1	8.7	25
(C1)	(−119.1)	(135.8)	(10)	(−87.3)	(104.1)	(15)
dissipating vortices:	−16.2	9.5	45	−12.8	9.8	54
symmetric cloud band (Da)	(−115.3)	(82.1)	(29)	(−95.5)	(80.5)	(32)
asymmetric cloud band	−23.2	13.8	4	−20.7	8.8	7
(Db)	(−140.5)	(77.8)	(2)	(−119.3)	(84.1)	(4)
decaying frontal vortex	−13.3	9.4	41	−10.5	9.3	49
(no cloud band: E)	(−161.7)	(74.8)	(18)	(−113.3)	(78.0)	(26)

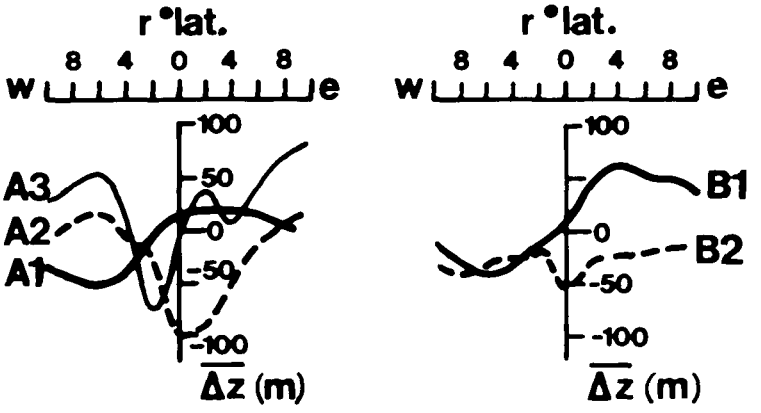

Fig. 9. West–east transects through each cloud vortex model type in October 1977 showing composite 850–700 mb thickness anomalies (m). The radial distances are measured in degrees of latitude out from the center (0°).

Fig. 10. Composite (all-latitudes) patterns of SLP and upper-air (500, 300 mb) height anomalies for cyclogenetic cloud vortex types in October 1977, derived from the procedure given in Fig. 5. The center of each grid (north at top) defines the mean satellite-observed center of the vortex. Each cross-hair is 10° latitude in length from the center. SLP anomalies are in millibars; 500- and 300-mb anomalies are in tens of meters.

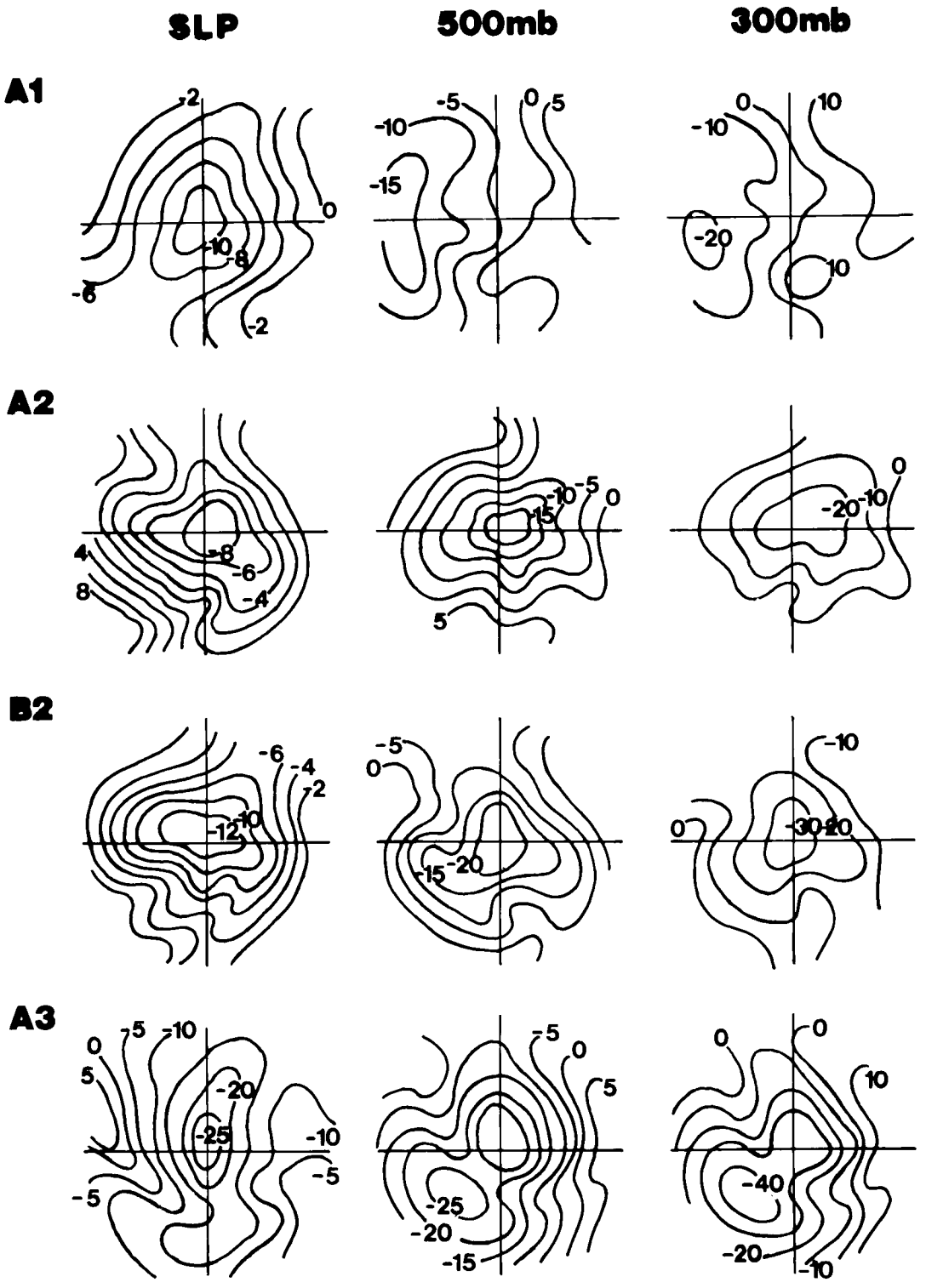
SLP
500mb
300mb
A1
A2
B2
A3

polar low vortex types, and are broadly consistent with those given for vortices in the southern hemisphere by Troup and Streten (1972). Models for October are presented here since the cloud vortex intensities are generally intermediate between those for summer (weakest) and winter (strongest), yet the basic spatial configurations are similar. The satellite-observed deformation of the cloud band characteristic of A1 is associated with a developing vorticity center at the surface. The anomalies are elongated along the approximate mean orientation of the cloud band. At the 500 and 300 mb levels (Fig. 10) there is a marked tilt of the vertical axis towards the cold air (west), and positive (warm) anomalies lie southeast of the mean center. In contrast, the smaller A2 vortex has a surface vorticity center located close to the satellite-observed location. These polar lows intensify strongly with height and there is little evidence of vertical tilt in the pressure/height minima (cf. A1). The mature polar low (B2) composite shows a similar pattern to A2 except that a lateral expansion of the system accompanies continued development (Fig. 10).

The surface anomaly patterns for the instant occlusion composite (Fig. 10) resemble, superficially, the mature and dissipating stages (C, D) of wave cyclones. However, the asymmetric pressure/height distribution implies a cyclogenetic process. Warm air advection occurs in the lower troposphere in association with the cloud band, and strong cold air intrusion is apparent to the west. At upper (500, 300 mb) levels, two distinct anomaly centers are present (Fig. 10), one apparently derived from the polar low, the other from the incipient frontal wave with which it has merged. This composite therefore lends support to the interpretation of instant occlusion development advanced by Locatelli et al. (1982) that the polar low supplies the vorticity center to the instant occlusion. In addition, this vortex type resembles the cyclogenesis described by Thepenier and Cruette (1981) and Zwatz-Meise and Hailzl (1983).

The relationship between anomalous atmospheric circulation conditions and the occurrence of polar lows in January 1979 is given in Fig. 11. The procedure for obtaining the satellite-observed cumulative negative height anomalies was given earlier (*Data and Methods of Analysis*, Subsection 4). Fig. 11 shows a major negative cumulative height anomaly (greater than −2760 m at 500 mb) north of the British Isles, and is

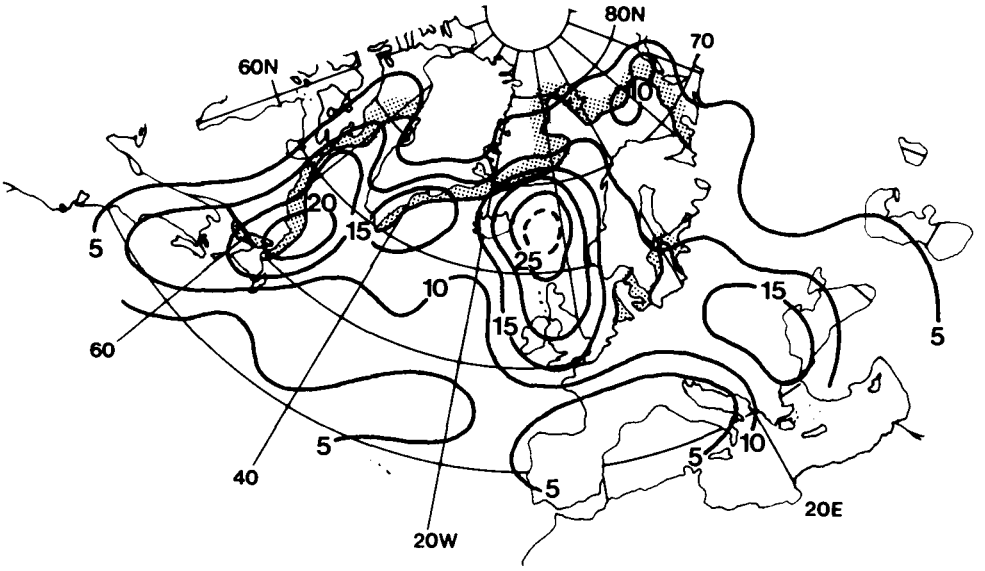

Fig. 11. Spatial pattern of cumulative 500 mb height anomalies ($\Sigma\overline{\Delta h}$) based on the frequencies of cloud vortex types for January 1979 (non-area normalized). Values are negative and in hundreds of meters. The location of the sea-ice margin at the end of that month is also shown.

associated with a surface pressure anomaly of greater than −300 mb (not shown). This deep cold anomaly is due predominantly to the large numbers of polar air vortices, relative to other types, observed in connection with the persistent northerly flow in that month. The Icelandic Low is correspondingly weaker than normal. Strong polar low activity is also contributing to the anomaly off the Labrador coast. This case result supports the link between seasonal climatic anomalies in the extratropics and the occurrence of polar lows, although analysis of additional years' data is clearly warranted.

5. Concluding remarks

The climatology presented in this paper confirms the prevalence of the polar low over the oceans in winter and the difference between the North Atlantic and North Pacific in terms of the relative frequencies of signature sub-types. The higher frequency of Rasmussen's spiraliform type in the North Atlantic seems to highlight the contribution of CISK to polar low development there. These lower-level thermal effects are implicit in the secondary maximum of polar-air vortex activity noted here in association with the winter sea ice margin of the Greenland/Norwegian seas, and which appears to manifest a synoptic surface to atmosphere feedback. Of course, analysis of further years' satellite data is required to verify these initial results.

Synoptic climatological models of polar lows, incipient frontal waves and instant occlusions reveal substantial differences in terms of surface pressure, upper-air height and lower tropospheric thickness departures. While the models are necessarily generalized, being averaged over all latitudes, they provide insight into the basic structure of and differences between extratropical cyclogenetic cloud vortex types. In contrast to the frontal wave, and as found in other recent studies (e.g. Forbes and Lottes, 1985), the polar low "comma cloud" is overall a cold-core system that intensifies aloft. The instant occlusion has structural similarities to both the frontal wave and comma cloud. The surface pressure anomalies associated with this vortex compare with those found for frontal vortices in their later (mature, dissipating) stages of evolution. However, the instant occlusion exhibits a somewhat asymmetrical pressure/height distribution that is indicative more of a cyclogenetic than occlusive process, at least in the mean. A cyclonic activity index related to cloud vortex frequency, type, statistical intensity, season and latitude of occurrence, is derived for the North Atlantic–Europe sector for January 1979. This case result supports the importance of polar air cyclogenesis during periods of anomalous extratropical circulation in winter. Continued examination of the large scale environments in which polar air vortices develop promises improved understanding of the contribution of meso-scale processes to cyclogenesis and its prediction numerically (Forbes, personal communication).

6. Acknowledgments

The various stages of this research were supported by National Science Foundation Division of Polar Programs grant NSF-DPP 7920853 to Drs. Roger Barry (CIRES) and H. J. Zwally (NASA), National Aeronautics and Space Administration Climate Program grant NAG-5-142 to Dr. Barry, and National Science Foundation Climate Dynamics Program grant ATM-76-20508. The DMSP imagery and sea ice data were made available through World Data Center-A for Glaciology (Snow and Ice), University of Colorado, Boulder. U.S. Navy "Spot" and NMC Climatological Grid-Point Data were obtained from the Data Support Section, National Center for Atmospheric Research (NCAR), Boulder, CO. I am grateful to Margaret Eccles (INSTAAR/CIRES, University of Colorado) for computing assistance, and to Professor Barry (CIRES).

REFERENCES

Carleton, A. M. 1979. A synoptic climatology of satellite-observed extratropical cyclone activity for the southern hemisphere winter. *Arch. Meteorol. Geophys. Bioklim. B2*, 265–279.

Carleton, A. M. 1981a. Climatology of the "instant occlusion" phenomenon for the southern hemisphere winter. *Mon. Wea. Rev. 109*, 177–181.

Carleton, A. M. 1981b. Monthly variability of satellite-

derived cyclonic activity for the southern hemisphere winter. *J. Climatol. 1*, 21–38.

Carleton, A. M. 1985. Synoptic cryosphere–atmosphere interactions in the northern hemisphere from DMSP image analysis. *Int. J. Remote Sensing 6*, 239–261.

Chang, D. T. and Sherr, P. E. 1969. Cloud pattern models for extratropical cyclogenesis. *Final Report, ESSA Contract E-203-68, Allied Research Associates Inc., Concord, Mass.* 146 pp.

Crutcher, H. L. and Meserve, J. M. 1970. *Selected level heights, temperatures, and dew points for the northern hemisphere.* NAVAIR 50-1C-52 (revised). Chief of Naval Operations, Washington, D.C. (January 1970).

Duncan, C. N. 1977. A numerical investigation of polar lows. *Q. J. R. Meteorol. Soc. 103*, 255–267.

Forbes, G. S. and Lottes, W. D. 1982. Characteristics and evolution of mesoscale cloud vortices occurring in polar airstreams, In: Preprint volume, *Conference on Cloud Physics*, November 15–18, 1982, Chicago, Ill. American Met. Soc., Boston, Mass. 310–311.

Forbes, G. S. and Lottes, W. D. 1985. Classification of mesoscale vortices in polar airstreams and the influence of the large-scale environment on their evolutions. *Tellus, 37A*, 132–155.

Gagnon, R. M. 1964. Types of winter energy budgets over the Norwegian Sea. *Publications in Meteorology, 64. Arctic Meteorology Research Group, Department of Meteorology, McGill University, Montreal.* 75 pp.

Harrold, T. W. and Browning, K. A. 1969. The polar low as a baroclinic disturbance. *Q. J. R. Meteorol. Soc. 95*, 710–723.

Houghton, D. M. 1958. Heat sources and sinks at the earth's surface. *Meteorol. Mag. 87*, 132–143.

Locatelli, J. D., Hobbs, P. V. and Werth, J. A. 1982. Mesoscale structures of vortices in polar air streams. *Mon. Wea. Rev. 110*, 1417–1433.

Lyall, I. T. 1972. The polar low over Britain. *Weather 27*, 378–391.

Mansfield, D. A. 1974. Polar lows: the development of baroclinic disturbances in cold air outbreaks. *Q. J. R. Meteorol. Soc. 100*, 541–554.

Mullen, S. L. 1979. An investigation of small-scale cyclones in polar air streams. *Mon. Wea. Rev. 107*, 1636–1647.

Mullen, S. L. 1983. Explosive cyclogenesis associated with cyclones in polar air streams. *Mon. Wea. Rev. 111*, 1537–1553.

Murty, T. S., McBean, G. A. and McKee, B. 1983. Explosive cyclogenesis over the northeast Pacific Ocean. *Mon. Wea. Rev. 111*, 1131–1135.

Oerlemans, J. 1980. A case study of a subsynoptic disturbance in a polar outbreak. *Q. J. R. Meteorol. Soc. 106*, 313–325.

Økland, H. 1976. An example of air mass transformation in the Arctic and connected disturbances of the wind field. *Report DM-20, Department of Meteorology, University of Stockholm, Sweden.* April 1976. 30 pp.

Økland, H. 1977. On the intensification of small-scale cyclones formed in very cold air masses heated by the ocean. *Institute Report Series No. 26, Universitetet i Oslo, Institutt for Geophysikk, August 1977.* 31 pp.

Rabbe, A. 1975. Arctic instability lows. *Meteorologiske Annaler 6*, 303. (Meteorologiske Institutt, Oslo).

Rasmussen, E. 1979. The polar low as an extratropical CISK disturbance. *Q. J. R. Meteorol. Soc. 105*, 531–549.

Rasmussen, E. 1981. An investigation of a polar low with a spiral cloud structure. *J. Atmos. Sci. 38*, 1785–1792.

Reed, R. J. 1979. Cyclogenesis in polar air streams. *Mon. Wea. Rev. 107*, 38–52.

Sanders, F. and Gyakum, J. R. 1980. Synoptic-dynamic climatology of the "bomb". *Mon. Wea. Rev. 108*, 1589–1606.

Sardie, J. M. and Warner, T. P. 1983. On the mechanism for the development of polar lows. *J. Atmos. Sci. 40*, 869–881.

Streten, N. A. 1975. Satellite derived inferences to some characteristics of the South Pacific atmospheric circulation association with the Niño event of 1972–73. *Mon. Wea. Rev. 103*, 989–995.

Streten, N. A. and Kellas, W. R. 1973. Aspects of cloud pattern signatures of depressions in maturity and decay. *J. Appl. Meteorol. 12*, 23–27.

Streten, N. A. and Troup, A. J. 1973. A synoptic climatology of satellite-observed cloud vortices over the southern hemisphere. *Q. J. R. Meteorol. Soc. 99*, 56–72.

Thepenier, R-M. and Cruette, D. 1981. Formation of cloud bands associated with the American subtropical jet stream and their interaction with midlatitude synoptic disturbances reaching Europe. *Mon. Wea. Rev. 109*, 2209–2220.

Troup, A. J. and Streten, N. A. 1972. Satellite-observed southern hemisphere cloud vortices in relation to conventional observations. *J. Appl. Meteorol. 11*, 909–917.

van Loon, H. and Rogers, J. C. 1978. The see-saw in winter temperatures between Greenland and Northern Europe. Part I: General description. *Mon. Wea. Rev. 106*, 296–310.

Widger, W. K. 1964. A synthesis of interpretations of extratropical vortex patterns as seen by TIROS. *Mon. Wea. Rev. 92*, 263–282.

Zick, C. 1983. Method and results of an analysis of comma cloud developments by means of vorticity fields from upper tropospheric satellite wind data. *Meteorol. Rundsch. 36*, 69–84.

Zwatz-Meise, V. and Hailzl, G. 1983. A cloud formation process contradictory to the classical occlusion development investigated with satellite images and model output parameters. *Arch. Meteorol. Geophys. Bioklim. A32*, 119–127.